International Research Journal of Engineering and Technology (IRJET) e-ISSN: 2395-0056
Volume: 07 Issue: 06 | June 2020 www.irjet.net p-ISSN: 2395-0072

ANALYSIS OF NORMALIZED DIFFERENCE IN WATER AND VEGETATION INDICES FROM SATELLITE IMAGERY

Miss. K. Sherin[1], Dr. G. Murugesan[2]

[1]*Student, Computer Science and Engineering, St.Joseph's College of Engineering, Tamilnadu, Chennai*

[2]*Professor, Computer Science and Engineering, St.Joseph's College of Engineering, Tamilnadu, Chennai*

Abstract - *Water being a prime natural resource and a basic human need. According to the recent survey, demand on water already exceeds supply to many parts of the world as the population grows. The main reason for the water crisis is low rainfall count all over the state. Scarcity of water has seen many reservoirs run dry. Global data documents the surface water and vegetation produces statistical information and satellite imagery. The Landsat images quantify the changes in surface water area at 30m resolution. The study in Madurantakam Lake analyzed the change in water area during a period of 2014 to 2019 using Sentinel 2 and Landsat 8 OLI images. Different indices like Normalized Difference Water and Vegetation index NDWI & NDVI were tested to extract the surface water area. The study shows that about 17.81 percent of drought level has increased during 2014 to 2016 and 23.82 percent of high water level has increased during 2017 to 2019.*

Key Words: **Satellite image, Water spread area, Occurrence, NDWI, NDVI**

1.INTRODUCTION

Modern Satellite technologies are used to collect huge volumes of Earth Observation data explained by Aseefa (2007) [1]. Nowadays, Water crisis has become a major problem all over the world. In a worldwide only about 14% of water use in domestic needs. Each day an individual requires a 2000-4000 litres of water will become a big challenge in future due to the rise of population. Rainfall in India is contingent on south-west monsoon and north-east monsoon. It is observed that 17 countries are water stressed in a recent survey. Water crisis in India has challenged an extent beyond Chennai which has surveyed recently the highest scarcity of water supply.

Remote Sensing is a technique that obtains information about an object or area by analysing the data acquired by the device. It defines the measurements of radio waves reflected from or emitted by a target from a point of view which is distant from the target. It is displayed as a necessary part of a huge information system. It acts as a key component for decision making in many applications. The multi-concept of remote sensing information consist of- Multi-station images, Multi-band images, Multi-date images, Multi-stage images, Multi-polarization images etc. The analysed data of spatial values are recovered by Geographic Information System. GIS handles the spatial data, contains unavoidable inputs from remote sensing. Satellite images provide useful information, which could be stored as record for future purpose. This technology offers a possibility to develop a compatible database at spatial, spectral and temporal resolution. The population increases day by day coercion on the natural resources. It is important to manage the available natural resources. Since, remote sensing technique provides information on Earth's surface uses unlimited applications. Collecting information on different application areas like agriculture, forestry, geography, geology, archaeology, weather and climate, marine environment, water resources management etc.

GIS is an essential supporting structure for gathering, managing and analysing data. Normally contemplate to involve spatial referenced computer database suitable application software. GIS needs spatial data making it unique. It describes the digital geographic data systematize as geographic database scales the data represented in different kinds of variables such as- Nominal, Ordinal, Interval and Ratio. GIS input data features both the spatial data and attribute data. The non-digital data (spatial data) are converted into digital form. This lake spreads over 2400 acres in Chengalpattu district, Tamil Nadu. The Chennai Metropolitan Area has nearly 4100 water bodies with a storage capacity of 150000 million cubic feet.

Stefan Voigt et al (2007), paper describes successful rapid satellite mapping campaigns supporting disaster relief and demonstrates how this technology can be used for civilian crisis-management purposes. This paper reflects on several of these international activities, such as the International Charter Space and Major Disasters, describes mapping procedures, and reports on rapid-mapping experiences gained during various disaster-response applications. Multiple satellite image processing and analysis techniques may successfully be applied individually or in a combined manor to serve rapid-mapping tasks in the domain of disaster and crisis-management support. During the analysis, response, and recovery phase, only very fast delivery of up-to-date, accurate, and comprehensive image analysis products can significantly help in the assessment of large disaster situations, in particular in remote areas, where other means of assessment or mapping either fail or are of insufficient quality.

Jose Don T. De Alban et al, (2018), paper discusses about processing, classification, sampling of satellite images for Analysis of combined Landsat and L-band SAR data provides an improved understanding of the associated drivers of agricultural plantation expansion and the dynamics of land use/cover change in tropical forest landscapes. Land cover classes are defined through a combination of field verification and visual interpretation of high-resolution imagery available from Google Earth Pro. A simple random sampling design to achieve our accuracy assessment objectives, which involves calculating unbiased accuracy and uncertainty estimates, was adopted.

Noel Gorelick et al (2017), This paper describes the Planetary-scale geospatial analysis with Google earth engine. Once an algorithm has been developed on Earth Engine, users can produce systematic data products or deploy interactive applications backed by Earth Engine's resources, without needing to be an expert in application development, web programming or HTML. The Earth Engine public data catalog is a multi-peta byte collection of widely used geospatial datasets.

The functions in the Earth Engine library utilize several built-in parallelization and data distribution models to achieve high performance. Each of these models is optimized for a different data access pattern. It is easy to access high-performance computing resources for processing very large geospatial datasets. Configuring large machines is not available, and there is a hard limit on this means that users can only express large computations by using the parallel processing primitives provided in the Earth Engine library and some non-parallelizable operations simply cannot be performed effectively in this environment. the amount of data that can be brought into any individual server.

Dániel Kristóf, (2014), this article describes various methods for preprocessing of satellite images. The major source for noise and inaccuracy was found to be Gridding. New polygon representation of MODIS observations has significantly increased correlation with same-day high resolution data: better representation of observation geometry. Data processing requires more computing power, but the user has full control over the process (thresholds, quality measures, etc.) and can obtain more accurate data with maximal spatial and temporal coverage.

Barry (2006), proposed a unique source of fresh water for agriculture, industry and domestic use, an important economic component, yet they constitute serious natural hazards. As glaciers are natural component, they are directly affected by small climatic fluctuations at both local as well as global level. Glacier length changes indicate the global climatic changes. The increasing mass loss and decline in glacier size in mountain and other regions contribute to sea level rise Larsen et al., 2007. The mass loss and change of length of glacier depends up on its geometry, and climatic variation. Various meteorological experiments have shown that the primary source for melting in glaciers is solar radiation, and loss of mass balance is due to temperature and precipitation.

Ninija Merina (2016) study describes the evaluation of sedimentation carried out for Vaigai reservoir. The capacity loss occurs in the reservoir due to sedimentation. As it is highly tedious and uneconomical to do hydrographic surveys, the frequentness in finding the sediment yield becomes impossible. The Satellite Remote Sensing (SRS) method for prediction of reservoir sedimentation uses directly the water-spread area of the reservoir at a particular elevation on the date of pass of the satellite. With known area and the difference in level of water, the capacity and thereby the loss in capacity of the reservoir due to sedimentation can also be estimated. A reservoir will generally be located towards the end of a large watershed and receives inflows from major rivers. Around 40,000 large reservoirs suffer from sedimentation and it is estimated that between 0.5% and 1% of the total storage capacity is lost per year. Periodically the capacity surveys the reservoir help in assessing the rate of sedimentation and reduction in storage capacity and calculates the quantity of sediment using remote sensing technology.

Jean-Francois Pekel and Andrew Cottam (2016) investigated their findings here reinforce the need for water-resource management strategies that integrate climate and socio-economic dimensions, has already been proposed. This analysis applies a consistent algorithm to all 32 years of the Landsat observations to produce a validated data set that documents global surface water dynamics with new levels of spatial detail and accuracy. Events such as lake expansion and retreat or river-channel migration provides insights into the impacts of climate change and climate oscillation on surface water distribution, and concurrently captures the impacts humans have on surface water resource distribution. The study collects and collates more than 3 million satellite images of Earth's surface taken over the past three decades, and shows how surface water rivers, lakes and wetlands has ebbed and flowed. More than 90,000 km^2 of water bodies thought to be permanent have disappeared including giant chunks of the Aral Sea and a further 72,000 km^2 is now classed as only seasonally flooded. But overall, there has been more flow onto the land than away from it: almost 213,000 km^2 of land that was dry.

Jan Eliasson (2016) said water is becoming scarcer as populations increase, potentially leading to conflict. Rapid urbanization is creating huge pressure on water use and infrastructure, with lasting consequences on human health and urban environments. Demand for water is projected to grow by more than 40% by 2050. Almost 750 million people do not have access to safe drinking water. Roughly 80% of wastewater is discharged untreated into oceans, rivers and

lakes. In 2015 and beyond, through efforts in diplomacy, economics and scientific research, we need to focus on water as a source of cooperation, rather than as a source of conflict.

Manish Kumar Dhasmana (2018) said during the study year 2017/18, the maximum reservoir level (508.64 m) was observed on September 20, 2017, which gradually reduced to minimum level of 467.38 on May 2, 2018. However, to cover the full extent of reservoir capacity i.e. from minimum reservoir level (467.38 m) to maximum reservoir level (511.32 m), one image for September 2015 was analysed. In this study, the cumulative revised capacity of the reservoir at lowest observed level (467.38m) was assumed to be same as the original cumulative capacity (1759.86) obtained from India-WRIS. The GobindSagar reservoir was first impounded in the year 1963 and the result from analysis of remote sensing approach shows that 783.38 Mm^3 of live storage have been lost in last 55 years (1963-2018). The mean sedimentation rate of GobindSagar reservoir comes out to be 14.24 Mm^3/year and capacity reduction of the reservoir is estimated to be 10.71%.

2. DATA AND TOOL USED

2.1 SATELLITE DATA

The global water risk mapping tool helps organizations, governments and other users to understand the severity on water risks. The Google Earth Engine tool elucidates various data sources from United States Geological Survey USGS collecting Landsat 8 OLI images. Spectral bands 1–8 of 30m per pixel resolution are layer-stacked to form a single image. It captures between 550-750 new images per day. The different dates of the satellite data that have been used are 20th September 2014, 22nd October 2015, 15th November 2016, 19th October 2017, 25th November 2018, and 23rd September 2019. Thus the validation of each result in surface water quality is collected from the official website of Tamil Nadu water project.

Similarly, all the vegetation datasets are collected from the MODIS data. As the equator over passes terra vegetation and land cover data are captured. The data provided here in 36 spectral bands with a resolution of 250,500 and 1000m. The satellite images are updated every five hours per day such that users obtain valid data. This obtains Normalized Difference in Vegetation Index (NDVI) and Enhanced Vegetation Index (EVI) for dense and sparse vegetation. By using this satellite image the entire planet can be viewed to get a better idea on vegetation and water that exist for years. Below diagram shows the system architecture of how the satellite imagery works in Google Earth Engine tool.

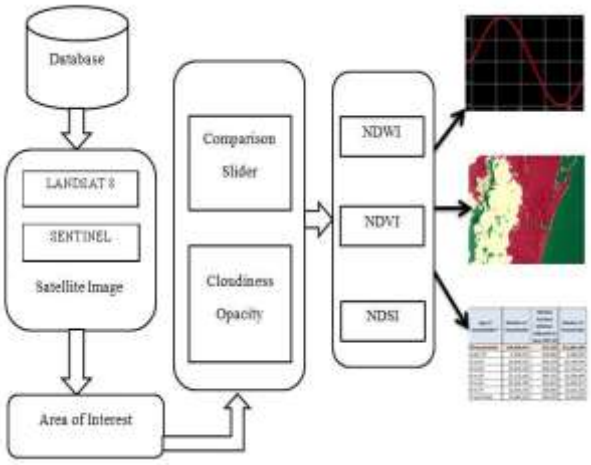

Fig- 2.1: System Architecture

2.2 DATA COLLECTION

The Earth Engine tool consist of multiple water related risk dataset. A set of dataset obtained in metadata are:

i. LANDSAT/LC08/C01/T1_TOA
ii. LANDSAT/LC08/C01/T1_SR
iii. JRC/GSW1_1/GlobalSurfaceWater
iv. NASA/GPM_L3/IMERG_V05
v. MODIS/006/MOD13A1

3. METHODOLOGY

This paper works with different approaches in surface water mapping through the following methods Area of interest (AOI), Change Detection, Comparison slider and Clustering of Normalized Difference in water index (NDWI) and Normalized Difference in Vegetation Index (NDVI).

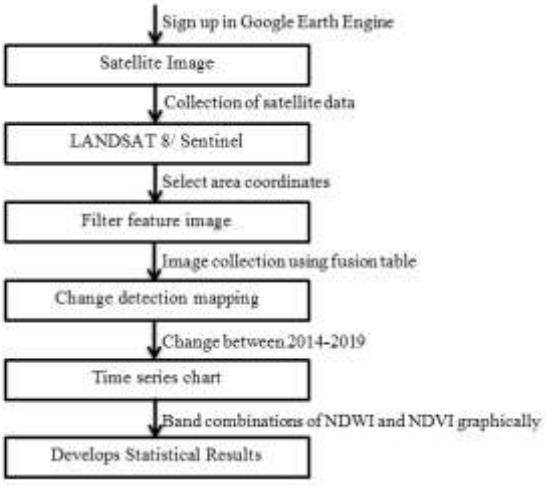

Fig-3: Flowchart

The surface water is estimated using a trapezoidal formula. The volume of the water spread area is estimated with

different dates with a period of five years using satellite image. The figure 3 shows the flowchart of calculating the water spread area.

3.1 FILTERING IMAGE COLLECTION

The Filtering image is used as an Earth Engine collection ID available in the fusion table. To, construct a particular image from a set of ID's and merge the existing collections. By, creating a random constant image obtaining a list to the constructor, merges the two image collections and attains a feature collection. Thus, maps a function by returning an image over a feature collection. In a simple way, the geometry points are marked for selecting a boundary of particular region. The coordinates of a region along with its zoom level is the syntax to select particular boundary region called feature collection. The watershed data are taken from the fusion table and computes its geometry area to add on to properties. The property list contains the measurement units and maps the function over features.

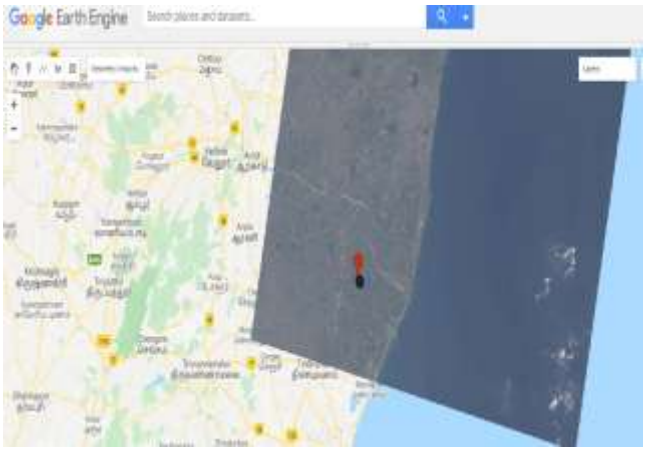

Fig- 3.1: Selected Region

3.2 CHANGE DETECTION

The process measures the attribute of a selected area that has changed between one or more time periods. It compares the satellite images taken at different times. The spatial representation of two points in time by controlling all variances caused by differences in variables that are not of interest and to measure changes caused by differences in the variables of interest. This method is carried away using two classification algorithms.

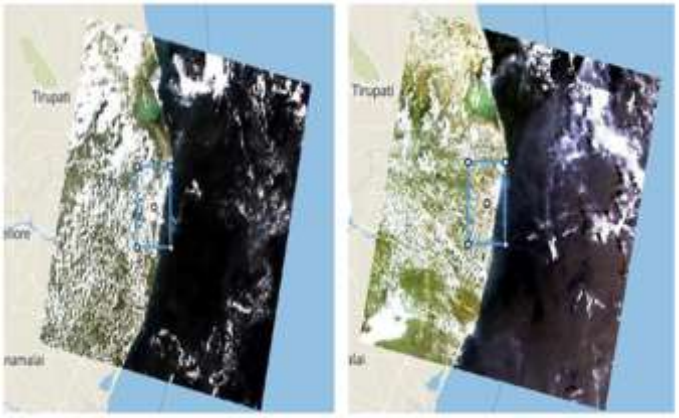

Fig-3.2: Change Detection between 2014 and 2019

The Supervised and Unsupervised Classification are the algorithms which trains the data which Collect training data. Assemble features which have a property that stores the known class label and properties storing numeric values for the predictors. Then instantiate the classifier and train the classifier using training data. Classify an image and estimate the error with independent validation data. A central application of unsupervised learning is in the field of density estimation in statistics, though unsupervised learning encompasses many other domains involving summarizing and explaining data features; unsupervised learning intends to infer an a prior probability distribution.

3.3 CLUSTERING

A statistical approach to band combinations NDVI and NDWI are carried away. The spectral indices values are calculated using Fuzzy C means algorithm. The pixel classification for the water spread area is multiplied by the selected area of the image pixel. The overall water spread area is estimated by reviewing the area occupied in each pixels proportion image.

$$Water\ spread\ area = \sum_{i=1}^{n} Prop_i * r^2$$

Where, n is the number of pixels and r is the resolution of satellite image.

These clustering method of spectral indices calculated for NDVI and NDWI are as follows,

$$NDVI = \frac{NIR - Red}{NIR + Red}$$

$$NDWI = \frac{Green - NIR}{Green + NIR}$$

3.4 TIME SERIES CHART

The Normalized water level and years are derived from the Satellite Image Time Series (SITS). This method detects

spatio-temporal entities and finally it characterizes their evolutions by mean of a graph-based representation. Clusters the drought level and high moisture content using the spectral indices occurs a graphical chart. Similarly, Normalized Vegetation are estimated to obtain sparse and dense vegetation.

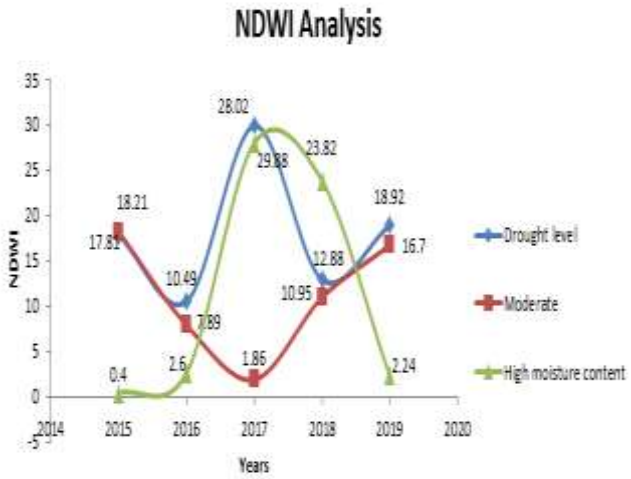

Fig- 3.4: Time series chart for NDWI

The Rate (%) normalized index value for water resources over six years is represented in a graphical format in figure 4.4.1. The period from 2014 to 2016 drought level increased by 17.81% and a hectare increase of 2516.07 ha Period of 2017 to 2019 drought increased by 12.88% and a hectare increase of 1818.85ha. Thus, the time period between 2014 and 2019 obtains an increase of 30.22%

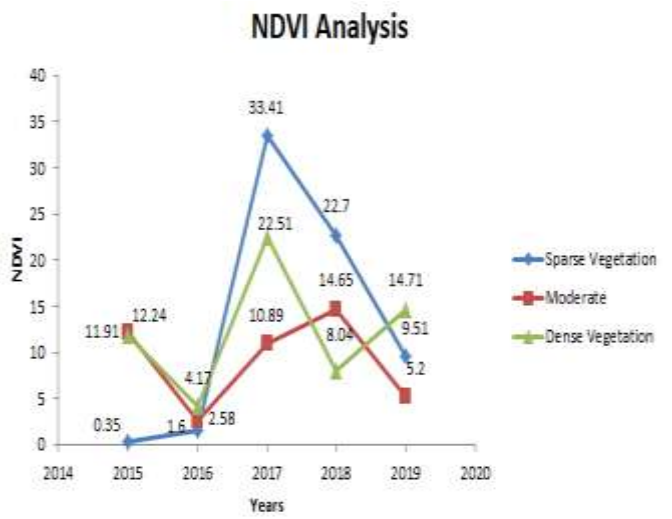

Fig- 3.4.1: Time series chart for NDVI

The Normalized vegetation results over a period from 2014 to 2016 sparse vegetation decreased by 0.35% and a hectare decrease of 48.59 ha whereas, the period from 2017 to 2019 dense increased by 22.7% and a hectare increase of 3206.78ha. The period from 2014 to 2019 obtains an increase of 0.05%. A complete graphical analysis of surface water spread change occurred in the year of 2019 is showed in figure 3.4.2 described below.

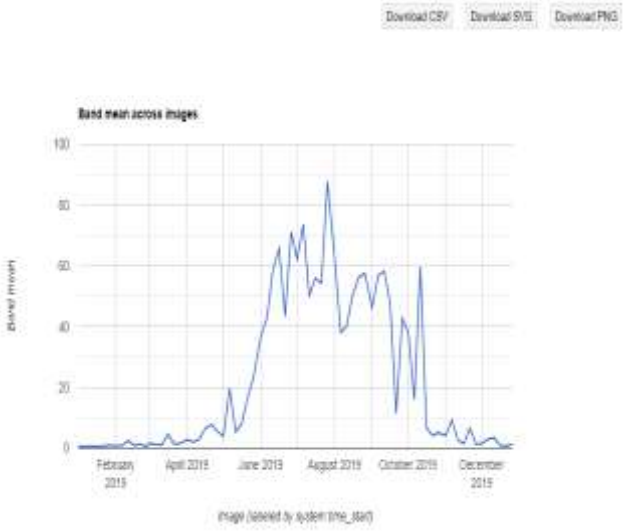

Fig-3.4.2: Graphical representation for one year of water occurrence

A statistical approach estimated through water analysis collects mean value of India every year from 2014 to 2019 which is described in the below figure 3.4.3

Fig- 3.4.3: Statistical result of water level from 2014 to 2019

4. RESULTS

In this paper the water spread area is estimated and analyses the severity of water risk for each area using the overall water risk indicators. It downloads a Meta data in spread sheet. A list of indicators for each location is displayed on the data sheet and obtains a statistical analysis of change in the reservoir.

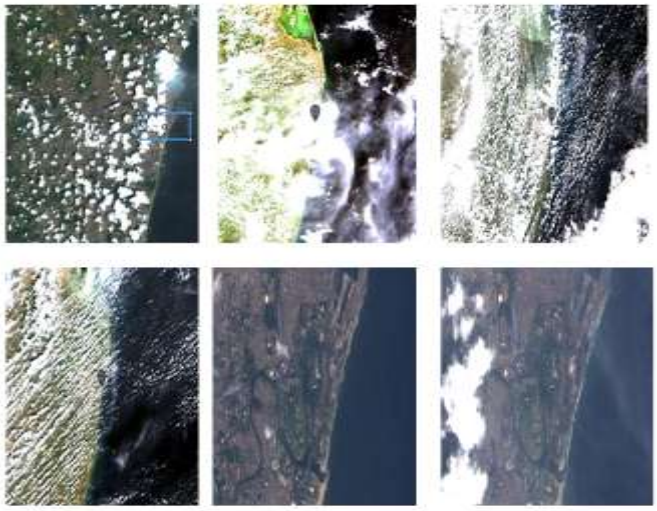

Fig- 4.1: LANDSAT image from Oct-2014, Oct-2015, Sept-2016, Nov-2017, Oct-2018 and Sept-2019

The above figure represents the Meta data of LANDSAT images from 20th September 2014, 22nd October 2015, 15th November 2016, 19th October 2017, 25th November 2018, and 23rd September 2019. The change occurrence values are obtained through water spread area calculation in the reservoir is described in figure 4.2 below

Table- 4.2: Estimated results obtained from NDWI and NDVI classes through spectral indices from 2014 to 2019

Classes	Spectral Indices	27th Oct 2014 (%)	17th Dec 2015 (%)	17th Nov 2016 (%)	4th Nov 2017 (%)	6th Oct 2018 (%)	23rd Sept 2019 (%)	Change Occurrence in 2014-2019 (%)
NDWI Classes	Drought level	8.96	26.77	37.26	7.38	20.26	39.18	30.22
	Moderate	75.47	57.26	49.37	51.23	62.18	45.48	29.99
	High moisture content	15.57	15.97	13.37	41.39	17.57	15.33	1.24
NDVI Classes	Sparse Vegetation	15.52	15.87	14.27	47.68	24.98	15.47	0.05
	Moderate	70.85	58.61	56.03	45.14	59.79	54.59	16.26
	Dense Vegetation	13.62	25.53	29.7	7.19	1523	29.94	16.32

5. CONCLUSION

A satellite image provides beneficial information on various wavelengths and maintains a record for future use. Remote sensing is advantageous for its large area coverage enabling regional surveys on identifying large features. With the help of Google Earth Engine tool the severity of water is analysed for every locations. This technique enables an easy collection of data on many scales. The global database and interactive tool that maps indicators of water-related risks are developed. Earth Engine enables comparison across large geographies to identify regions or assets deserving of closer attention. The water risk framework functions the metrics and generates an aggregated score. The scarcity on water can be reduced if little effort taken by the population to safeguard water for the future use. Few precautions that could be taken to avoid the scarcity are as follows, Efficient Irrigation- In order to restraint the problem on baseline water stress countries must shift to better planned irrigation technologies.

Conservation of water- Promote the conservation and storage of water bodies like lakes, ponds, freshwaters, rainfall etc., to avoid scarcity in groundwater crisis.

Water-related data- India can manage its water risk with the help of dependable and vigorous data concern to rainfall, surface, and groundwater to develop strategies that strengthen resilience.

REFERENCES

[1] Aseefa, Jose Don T. De Alban, Grant M. Connette, Patrick Oswald and Edward L. Webb (2018) "Combined Landsat and L-Band SAR Data Improves Land Cover Classification and Change Detection in Dynamic Tropical Landscapes", Remote Sensing, Vol. 10, No. 2.

[2] Stefan Voigt, Thomas Kemper, Torsten Riedlinger, Ralph Kiefl, Klaas Scholte, and Harald Mehl, (2007) "Satellite Image Analysis for Disaster and Crisis-Management Support" , IEEE on Geoscience and Remote Sensing Vol. 45, No.6, pp.1520–1528

[3] Anmin Fu, Guoqing Sun, Zhifeng guo, Dianzhong Wang (2010), "Forest cover classification from MODIS images in north eastern asia", Earth Observation and Remote Sensing Applictions, Vol.3, No.12.

[4] Azad Rasul (2018), "Using Landsat 8 images along with Google Earth Engine for investigation the location of the crashed aircrafts" Remote Sensing Technology, Vol. 1, No. 3.

[5] Daniel Kristof (2014), "Satellite data processing and analysis", International LCLUC Regional Science Meeting, Vol. 10, No. 5.

[6] Noel Gorelick, Matt Hancher, Mike Dixonb, Simon Ilyushchenko, David Thaub, Rebecca Moore (2017) "Google Earth Engine: Planetary-scale geospatial analysis for everyone", Remote sensing of Environment, Vol.10, No. 13.

[7] G. Trianni, E. Angiuli, G. Lisini, P. Gamba (2014) "Human settlements from Landsat data using Google Earth Engine" IEEE IGARSS, Vol. 5, No. 12.

[8] Barry. R.G (2006) "The status of research on glaciers and global glacier recession: a review". Progress in Physical Geography, Vol. 30, No.3, pp. 285-306.

[9] Ninija Merina, Sashikkumar. R, Rizvana. M. C, Adlin. N (2016) "Sedimentation Study In A Reservoir Using Remote Sensing Technique" in Applied Ecology and Environmental Research Vol.14, No.4, pp. 296-304.

[10] Alan Belward. S, Andrew Cottam, Jean-Francois Pekel and Noel Gorelick (2016), "High-resolution mapping of global surface water and its long-term changes" Research Letter, Springer Nature, pp.1-19.

[11] Jan Eliasson (2019) "The rising pressure of global water shortages" Nature Research Journal, Vol. 517, No. 6, pp. 45-55.

[12] Manish Kumar Dhasmana, Sachchidanand Singh, Vaibhav Shrivastava and Vishal Sharma (2018) "Estimation of Revised Capacity In GobindSagar Reservoir Using Google Earth Engine And Gis The International Archives of the Photogrammetry, Remote Sensing and Spatial Information Sciences", ISPRS TC V Mid-term Symposium "Geospatial Technology – Pixel to People", Vol. XLII, No. 5, pp.20–23.